Colorimetric sensing of Cu(II): Cu(II) induced deprotonation of an amide responsible for color changes†

Shu-Pao Wu,* Kun-Ju Du and Yi-Ming Sung

Received 10th December 2009, Accepted 18th March 2010
First published as an Advance Article on the web 8th April 2010
DOI: 10.1039/b925898a

9,10-Anthraquinone-based chemosensor **1** indicates the presence of Cu(II) ions among other transition metal ions with high selectivity by a color change from yellow to dark red. Chemosensor **2** shows binding toward Cu(II), Ni(II) and Co(II) with color changes from yellow to dark red, red and pale green, respectively. Especially, Co(II) binding with chemosensor **2** causes significantly green fluorescence. On addition of Cu(II), **1** and **2** exhibit 76 and 80 nm red shifts in absorption wavelength (pH 7.0). The effect on pH by the formation of these **1**-Cu(II) and **2**-Cu(II) complexes was determined by UV-vis spectroscopic pH titration. In the pH range of 6–7.5, a maximum absorption was observed at 473 nm and exhibited the formation of deprotonated **1**-Cu(II) and **2**-Cu(II) complexes.

Introduction

In recent years, an intense effort has been placed on the development of molecular devices for metal ion detection. The most common approach to the development of metal ion chemosensors is to connect a metal-binding unit with a signaling unit such as a chromophore or a fluorophore. The presence of metal ions causes a signal during interactions with binding units that results in a change in absorption wavelength or emission intensity.[1] A metal ion chemosensor can be viewed as a metal-binding ligand. Metal ion chemosensors can selectively bind a specific metal ion or have a higher binding affinity towards a metal ion.

Among the first row transition metal ions, Cu(II) and Zn(II) are two of the most frequently studied metal ions in the area of chemosensors.[2,3] Only a few chemosensors have been developed for Fe(III), Co(II) and Ni(II) due to their low binding affinity with a given ligand.[4,5] According to the Irving–Williams series, out of the first row transition metal ions, Cu(II) has the greatest formation constant with ligands containing oxygen or nitrogen donor atoms.[6] This is a great advantage when considering the design of Cu(II) chemosensors. To distinguish Cu(II) ions from other metal ions, a chemosensor must be designed with a suitable binding affinity toward metal ions. In other words, a Cu(II) chemosensor is a "poor" ligand, which only binds Cu(II) ions or has a significantly higher binding affinity with Cu(II) ions than with other metal ions.

Cu(II) recognition is also a key issue for the design of Cu(II) chemosensors. Cu(II) can induce deprotonation of the NH amide or NH groups that are conjugated to aromatic compounds upon Cu(II) binding. This deprotonation process caused by Cu(II) binding can be used for Cu(II) recognition. In addition, Cu(II)-induced deprotonation of NH groups that are conjugated to aromatic compounds, such as 1,4-naphthoquinone[2f] and 9,10-anthraquinone,[2f,2g] causes an internal charge transfer (ICT), which can be observed as a shift in absorption wavelength or color change. This color change mechanism has recently been applied for highly selective Cu(II) detection.

In this study, two 9,10-anthraquinone-based chemosensors (chemosensors **1** and **2**, see Scheme 1) were designed for metal ion detection. The 9,10-anthraquinone moiety has recently been used as a signal unit for sensing metal ions and anions because its optical properties can be significantly perturbed by chemical stimuli.[2f,2g,7,8] Both chemosensors contain an amide attached to a 9,10-anthraquinone moiety and function as chelating agents that are able to form complexes with metal ions. The only difference is the ring in the metal-chelating ligand: chemosensor **1** contains a benzene ring and chemosensor **2** contains a pyridine ring. This difference results in chemosensors **1** and **2** exhibiting different metal ion selectivity. Chemosensor **1** shows highly selective binding with Cu(II), resulting in a pronounced color change from yellow to red. Chemosensor **2** shows binding toward Cu(II), Ni(II) and Co(II) with a color change from yellow to dark red, red and pale green, respectively. In particular, Co(II) binding with chemosensor **2** causes significant green emission. The pH titration experiments on Cu(II) binding with chemosensors **1** and **2** revealed that the color change upon Cu(II) binding was primarily due

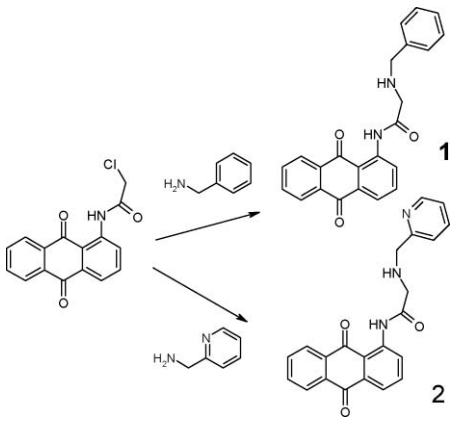

Scheme 1 Synthesis of chemosensors **1** and **2**.

Department of Applied Chemistry, National Chiao Tung University, Hsinchu, Taiwan, Republic of China. E-mail: spwu@mail.nctu.edu.tw; Fax: +886 3 5723764; Tel: +886 3 5712121-ext 56506

† Electronic supplementary information (ESI) available: Fluorescence, absorbance and IR spectra, Job plots and pH titrations. See DOI: 10.1039/b925898a

to the deprotonation of the amide group attached to 9,10-anthraquinone.

Results and discussion

Synthesis of chemosensor 1 and 2

The procedure for the synthesis of chemosensor **1** and **2** is shown in Scheme 1. 1-(Chloroacetylamido)-anthracene-9,10-dione was reacted with benzylamine or aminomethylpyridine to form chemosensors **1** and **2**, respectively. These products were purified using column chromatography with a 1 : 5 ethyl acetate–hexane eluent and subsequently characterized using mass and NMR spectrometry. The structures of chemosensors **1** and **2** are similar; the only difference is the ring in the metal-chelating ligand. Chemosensor **1** contains a benzene ring while chemosensor **2** contains a pyridine ring. Both chemosensors are yellow with a maximum absorption wavelength at 397 nm and exhibit weak fluorescence ($\lambda_{em} = 505$ nm, $\Phi = 0.002$).

Spectrophotometric estimation of Cu(II) binding with chemosensors 1 and 2

The ability of chemosensor **1** to form complexes with metal ions was first studied using ultraviolet-visible (UV-vis) spectroscopy. Metal ions including Ca^{2+}, Cd^{2+}, Co^{2+}, Cu^{2+}, Fe^{2+}, Fe^{3+}, Hg^{2+}, Mg^{2+}, Mn^{2+}, Ni^{2+} and Zn^{2+} were tested using chemosensor **1** for ion detection. The UV-vis spectra resulting from the introduction of various metal ions are presented in Fig. 1. For chemosensor **1**, Cu^{2+} was unique in producing a 76 nm red-shift (from 397 to 473 nm), which resulted in a visible color change from yellow to dark red (see Fig. 1). Competitive experiments were carried out in the presence of Cu^{2+} with other metal ions (Fig. 2). The absorption change at 473 nm caused by the mixture of Cu^{2+} with the other metal ion was similar to that caused by only Cu^{2+}. This indicates that other metal ions did not interfere with the binding of chemosensor **1** with Cu^{2+}. These observations indicate that Cu^{2+} is the only ion readily bound with chemosensor **1** to induce a color change from yellow to dark red, permitting highly selective detection of Cu^{2+}.

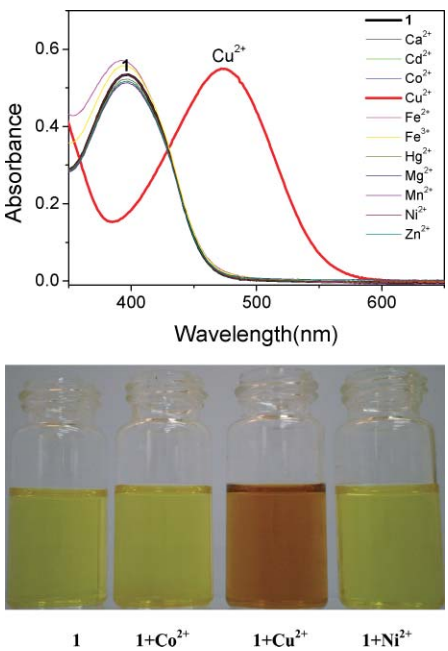

Fig. 1 (Top) Absorption change in the UV-vis spectra of chemosensor **1** (black line, 100 μM) upon the addition of metal ions (100 μM) in a methanol–H_2O solution (v/v = 4 : 1, 20 mM Hepes buffer, pH 7.0). (Bottom) Color of chemosensor **1** (100 μM) before and after the addition of metal ions (100 μM) in a methanol–H_2O solution (v/v = 4 : 1, 20 mM Hepes buffer, pH 7.0).

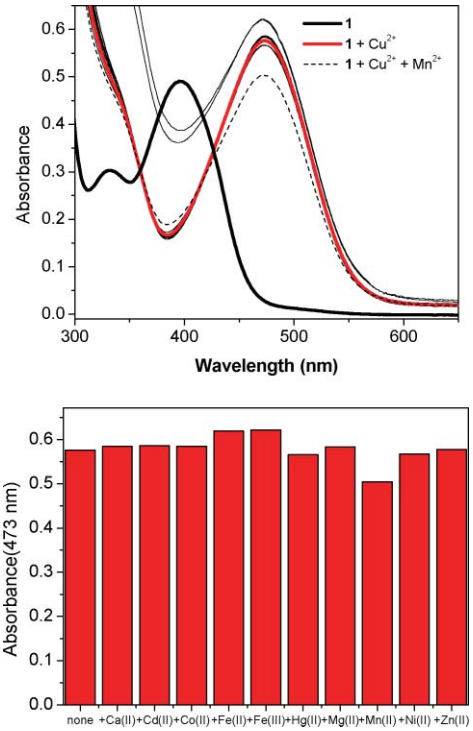

Fig. 2 (Top) UV-vis absorption response of chemosensor **1** (black line, 100 μM) to Cu^{2+}(200 μM) over the selected metal ions (200 μM) in a methanol–H_2O solution (v/v = 4 : 1, 20 mM Hepes buffer, pH 7.0). (Bottom) Absorbance at 473 nm upon the addition of chemosensor **1** to Cu^{2+} over the selected metal ions.

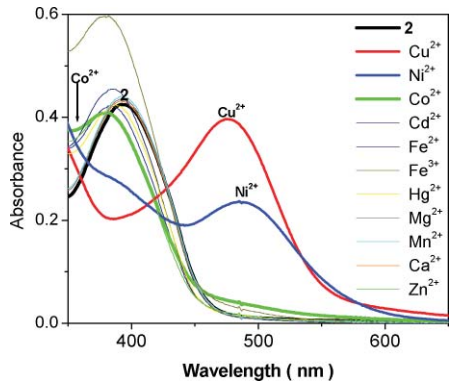

Fig. 3 Absorption change in the UV-vis spectra of chemosensor **2** (black line, 100 μM) upon the addition of metal ions (100 μM) in a methanol–H_2O solution (v/v = 4 : 1, 20 mM Hepes buffer, pH 7.0).

The ability of chemosensor **2** to form complexes with metal ions was also studied using UV-vis spectroscopy (Fig. 3). The addition

of Cu^{2+} to chemosensor **2** caused an 80 nm red-shift (from 397 to 477 nm), which resulted in a color change from yellow to dark red. This observation is similar to that of the addition of Cu^{2+} to chemosensor **1**. Cu^{2+} binding with chemosensors **1** and **2** caused an almost identical red-shift and color change. Addition of Ni^{2+} to chemosensor **2** caused an 86 nm red-shift (from 397 to 483 nm), which resulted in a color change from yellow to red (Fig. 4). The addition of Co^{2+} to chemosensor **2** resulted in a blue-shift and a color change from yellow to pale green, resulting in significant green light emission (Fig. 4). Chemosensor **2** shows less selective detection of metal ions such as Cu^{2+}, Ni^{2+}, and Co^{2+}.

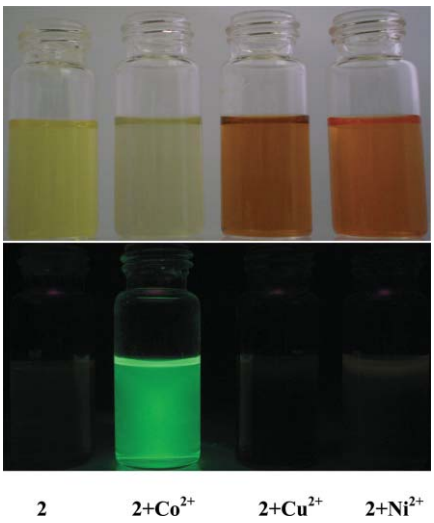

Fig. 4 Color (top) and fluorescence (bottom) of chemosensor **2** (100 μM) before and after the addition of metal ions (100 μM) in a methanol–H_2O solution (v/v = 4 : 1, 20 mM Hepes buffer, pH 7.0).

The ability of chemosensors **1** and **2** to form complexes with metal ions was also studied using fluorescence spectroscopy. For chemosensor **1**, Cu^{2+} was the only metal ion which resulted in significant fluorescence quenching (see Fig. S1 in the ESI†). Other metal ions only caused minor changes in fluorescence intensity. Chemosensor **1** detected Cu^{2+} through a fluorescence quenching process which arises from an energy or charge transfer mechanism.[2k] Co^{2+} binding with chemosensor **2** resulted in a significant increase in fluorescence intensity (Fig. 5), while other metal ions only caused a small change in fluorescence intensity.

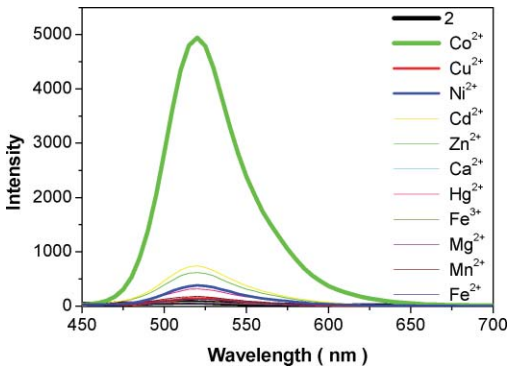

Fig. 5 Fluorescence spectra of chemosensor **2** (100 μM) in a methanol–H_2O solution (v/v = 4 : 1, 20 mM Hepes buffer, pH 7.0) in the presence of different metal ions (100 μM).

The quantum yield of **2**-Co^{2+} complexes was determined as 0.242, which is 100-fold higher than that of chemosensor **2**, at 0.002. This demonstrated that chemosensor **2** can detect Co^{2+}, yielding a significant increase in fluorescence. The mechanism of fluorescence of **2**-Co^{2+} complexes is based on CHEF (chelation-enhanced fluorescence) of 1-amino-9,10-anthraquinone.[9] Competitive experiments were carried out in the presence of Co^{2+} with other metal ions (Fig. 6). Emission intensity at 520 nm caused by Co^{2+} was completely quenched in the presence of Cu^{2+}. This indicates that Cu^{2+} dominated binding with chemosensor **2** and resulted in low emission intensity. In the presence of Ni^{2+}, emission intensity reached half the intensity of Co^{2+}-**2** complexes. This observation indicates that Ni^{2+} and Co^{2+} competed to bind with chemosensor **2**. In addition, the colors of the metal ion mixture with chemosensor **2** depended on the composition. In the presence of Cu^{2+}, the color was dark red and no green light emission was observed. In the presence of Ni^{2+}, the color was red and weak green light emission was observed. These findings indicated that Cu^{2+} dominates binding with chemosensor **2** followed by Ni^{2+}. This observation is consistent with the Irving–Williams series, in which

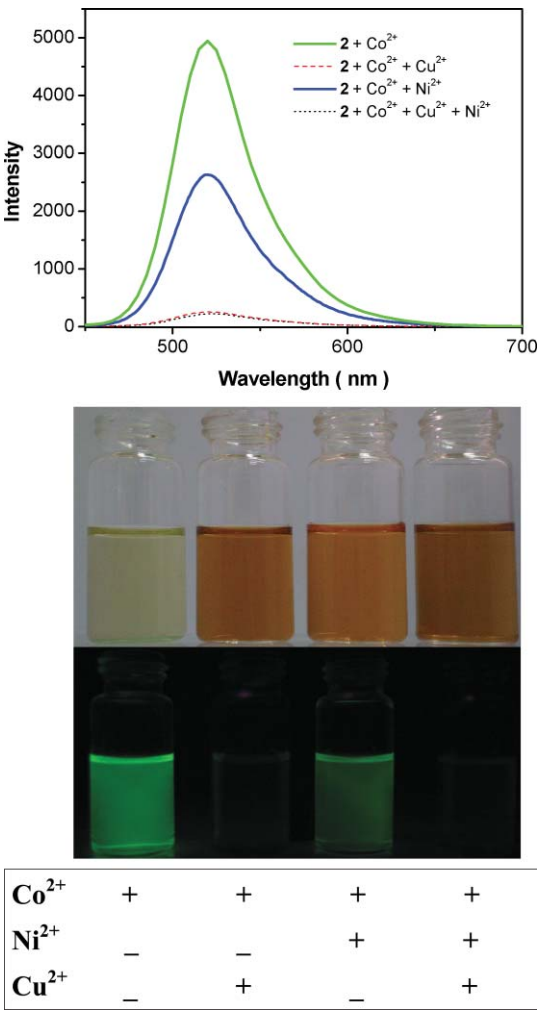

Fig. 6 (Top) Fluorescence spectra of chemosensor **2** (100 μM) after the addition of metal ions (200 μM) in a methanol–H_2O solution (v/v = 4 : 1, 20 mM buffer). (Bottom) Color and emission of chemosensor **2** in the presence of the mixture of metal ions.

Cu(II) has the highest formation constant with ligands among the first row transition metal ions.

Stoichiometries and affinity constants of 1-Cu^{2+} and 2-Cu^{2+}

The binding stoichiometry of **1**-Cu^{2+} and **2**-Cu^{2+} complexes was determined using Job's plot experiments.[10] In Fig. 7, the absorbance at 473 nm was plotted against the molar fraction of both chemosensors under a constant total concentration. A maximum absorbance was observed when the molar fraction was 0.5, which indicates a 1 : 1 ratio for both the **1**-Cu^{2+} and **2**-Cu^{2+} complexes. The association constant, K_a, was evaluated graphically by plotting $1/\Delta A$ against $1/[Cu^{2+}]$ as shown in Fig. 8. The data was linearly fit according to the Benesi–Hilderbrand equation and a K_a value was obtained from the slope and intercept of the line.[9] The K_a values obtained for **1**-Cu^{2+} and **2**-Cu^{2+} complexes were 8470 and 18667 M^{-1}, respectively. For Cu^{2+} binding, chemosensor **2** has a two-fold higher association constant than chemosensor **1**. This is due to the extra coordination nitrogen in the pyridine ring. The binding stoichiometry of the **2**-Ni^{2+} and **2**-Co^{2+} complexes was also determined using Job's plot experiments (see Fig. S2 in the ESI†). The **2**-Ni^{2+} complex has a maximum point at 0.6, which indicates two possible ratios (**2**/Ni^{2+}), 1 : 1 and 2 : 1. The **2**-Co^{2+} complex has a maximum point at 0.4, which indicates two possible ratios (**2**/Co^{2+}), 1 : 1 and 1 : 2, for **2**-Co^{2+} complexes.

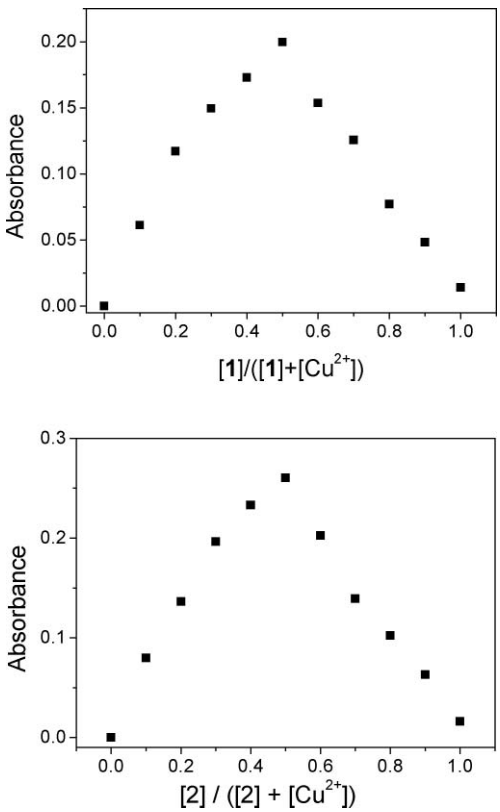

Fig. 7 Job's plot of a 1 : 1 complex of **1**-Cu^{2+} (top) and **2**-Cu^{2+} (bottom), where the absorbance at 473 nm was plotted against the mole fraction of Cu^{2+} at a constant total concentration of 1.0×10^{-4} M in a methanol–H_2O solution (v/v = 4 : 1, 20 mM Hepes buffer, pH 7.0).

To demonstrate the Cu^{2+}-induced deprotonation of the amide group in chemosensor **1**, pH titration experiments were carried

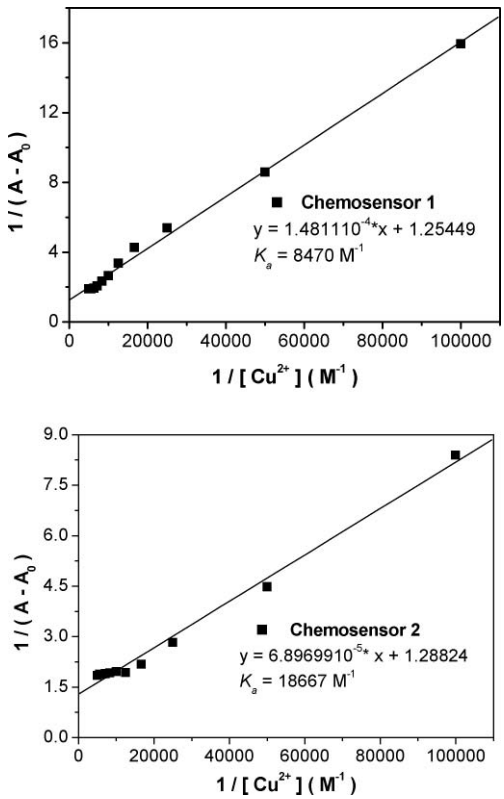

Fig. 8 Benesi–Hilderbrand plot of chemosensor **1** (top) and chemosensor **2** (bottom) with $Cu(BF_4)_2$.

out. First, the influence of pH on chemosensor **1** was studied using UV-vis spectroscopy (see Fig. S3 in the ESI†). Over a pH range of 6–10, the visible absorption band centered at 397 nm was unchanged. A decrease in pH from 5.5 to 1 engendered a shift in the maximum absorption wavelength to 390 nm; this 7 nm shift was due to protonation of the amide group. The effect of pH on Cu^{2+} binding to chemosensor **1** was further studied by monitoring red **1**-Cu^{2+} complexes at a wavelength of 473 nm (see Fig. 9). The absorbance at this wavelength suddenly increased at pH 6.0 and reached a maximum over a pH range of 6.0–7.5 for chemosensor **1**. This indicates that the formation of red **1**-Cu^{2+} complexes is a deprotonation process. When the pH value exceeded 8, the absorbance at 473 nm gradually decreased. This was due to the dissociation of red **1**-Cu^{2+} complexes, which resulted in lower absorbance at 473 nm. At pH values less than 4, absorbance was almost negligible; evidently the **1**-Cu^{2+} complexes do not exist over this pH range. For chemosensor **2**, there were two flat areas in the pH range of 3.5–5.5 and 6.0–10.0. The first flat area (pH 3.5–5.5) indicated the formation of non-deprotonated **2**-Cu^{2+} complexes. The second flat area (pH 6.0–10.0) represented the formation of deprotonated **2**-Cu^{2+} complexes. This observation differed from that of chemosensor **1**. The deprotonated **1**-Cu^{2+} complexes were gradually decomposed at pH > 8, but the deprotonated **2**-Cu^{2+} complexes were stable at pH > 8.

The effect of pH on the formation of **2**-Ni^{2+} and **2**-Co^{2+} complexes was also studied (see Fig. S5 in the ESI†). For **2**-Ni^{2+} complexes, the absorbance at the wavelength 479 nm abruptly increased at pH 6.0 and reached a maximum at pH 8.0. This indicates that the formation of red **2**-Ni^{2+} complexes is

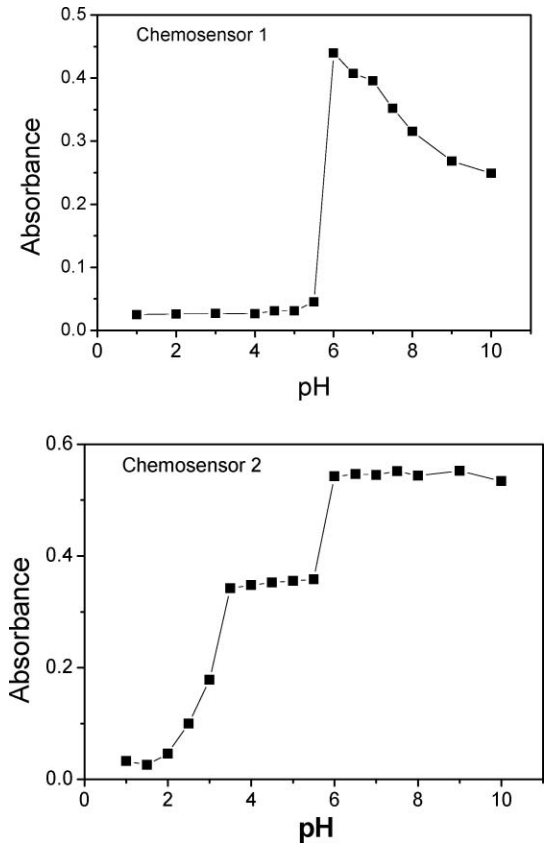

Fig. 9 pH titration of Cu^{2+} (10^{-4} M) bonded with chemosensor **1** (top) and chemosensor **2** (bottom) (10^{-4} M) in a methanol–H_2O solution (v/v = 4 : 1, 20 mM buffer). The absorbance at 473 nm was plotted against pH.

a deprotonation process. When the pH value exceeded 8, the absorbance at 479 nm gradually decreased, due to the dissociation of red **2**-Ni^{2+} complexes. For the **2**-Co^{2+} complexes, the emission at the wavelength 520 nm increased sharply at pH 6.5, and reached a maximum at pH 7.5. This also indicates that the formation of **2**-Co^{2+} complexes is a deprotonation process.

To gain a clearer understanding of the structure of **1**-Cu^{2+} complexes, Infrared (IR) spectroscopy was employed. The IR spectra were primarily characterized by bands in the carbonyl region. Two bands, 1666 and 1652 cm^{-1}, were associated with C=O absorption in the amide and quinone components of chemosensor **1** (see Fig. S6 in the ESI†). Binding of Cu^{2+} with chemosensor **1** resulted in a shift in the carbonyl region peaks to 1660 and 1626 cm^{-1}. The significant shift observed in the carbonyl absorption band from 1652 to 1626 cm^{-1} was due to Cu^{2+}-induced deprotonation of the amide group during binding.[11] The downward shift in the IR spectrum from 1666 to 1660 cm^{-1} was indicative of direct interaction between Cu^{2+} and the anthracene-9,10-dione oxygen.[12] Chemosensor **1** thus forms a tridentate ligand in which Cu^{2+} is bound with two nitrogens and one oxygen in anthraquinone. This model is consistent with previous indications that Cu^{2+} ions form a 1 : 1 ratio complex with chemosensor **1** (Scheme 2). The IR spectra of **2**-Cu^{2+} complexes is similar to that of **1**-Cu^{2+} complexes. Binding of Cu^{2+} with chemosensor **2** resulted in a shift in the carbonyl region from 1651 to 1645 cm^{-1} and from 1679 to 1670 cm^{-1}. This indicated that Cu^{2+} bonded with chemosensor **2** through the carbonyl oxygen in anthraquinone.

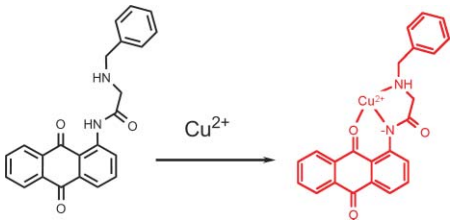

Scheme 2 A bonding model of the **1**-Cu^{2+} complex.

Conclusions

In summary, two 9,10-anthraquinone-based colorimetric chemosensors have been developed for Cu^{2+} detection. Chemosensor **1** functions as a chelating agent that binds a Cu^{2+} ion through three functional groups: amine nitrogen, amide nitrogen and quinone oxygen. The Cu^{2+} binding of chemosensor **1** induces deprotonation of the amide group and results in a significant color change from yellow to dark red, with a 76 nm red-shift. Chemosensor **2** can detect Cu(II), Ni(II) and Co(II) with a color change from yellow to dark red, red and pale green, respectively. In particular, Co(II) binding with chemosensor **2** causes significantly green fluorescence.

Experimental

Materials and instrumentations

All solvents and reagents were obtained from commercial sources and used as received without further purification. UV-vis spectra were recorded on an Agilent 8453 UV-vis spectrometer. Fluorescence spectra were recorded in a Hitachi F-4500 spectrometer. IR data were obtained on Bomem DA8.3 Fourier-Transform Infrared Spectrometer. NMR spectra were obtained on a Bruker DRX-300 NMR spectrometer.

Synthesis of chemosensor 1 and chemosensor 2. The reaction mixture containing 1-(chloroacetylamido)-anthracene-9,10-dione[8] (299.0 mg, 1.0 mmol), triethylamine (0.696 mL, 5.0 mmol), potassium iodide (10 mg) and 5.0 mmol benzylamine (or aminomethylpyridine) in THF was heated for 14 h at 60 °C. After cooling, the solvent was removed by rotor vacuum and dichloromethane was added to dissolve the reaction mixture. Product was separated in silica gel by eluting with ethyl acetate–hexane = 1 : 5. Yellow band was collected and the yields of **1** and **2** were 67% and 74%, according to the amount of 1-chloroacetylamido-anthracene-9,10-dione.

Chemosensor 1. EI-Mass *m/z* (%): 91 (100), 106 (47.6), 120 (65.1), 223 (46.4), 251 (35), 265 (5.3), 371 (2.3). HRMS(EI) *m/z* calcd for $C_{23}H_{18}N_2O_3$, 370.1317, found, 370.1317. ^{1}H-NMR(300 MHz, $CDCl_3$):δ 13.06 (1H, s), 9.10 (1H, d, 8.2 Hz), 8.14–8.22 (2H, m), 7.95 (1H, d, 7.2 Hz), 7.64–7.72 (3H, m), 7.45 (2H, d, 7.2 Hz), 7.29 (2H, t, 7.2 Hz), 7.20 (1H, t, 7.2 Hz), 3.88 (2H, s), 3.49 (2H, s).^{13}C-NMR (100 MHz, $CDCl_3$):δ 186.9, 183.2, 172.8, 141.7, 139.7, 135.9, 134.7, 134.6, 134.5, 134.4, 133.2, 128.9, 128.8, 127.8, 127.7, 127.4, 126.7, 123.1, 118.7, 54.5, 53.9.

Chemosensor 2. EI-Mass *m/z* (%): 92(100.0), 107(15.1), 119(80.5), 221(6.5), 251(3.9), 371(1.1). HRMS *m/z* calcd for $C_{22}H_{17}N_3O_3$ = 370.1270, found, 370.1284. ^{1}H-NMR (300 MHz,

$CDCl_3$) δ 13.23 (1H, s), 9.24 (1H, d, 8.6 Hz), 8.61 (1H, d, 4.8 Hz), 8.29 (2H, t, 4.5 Hz), 8.10 (1H, d, 7.5 Hz), 7.76–7.84 (3H, m), 7.77 (1H, t, 7.6 Hz), 7.50 (1H, d, 7.8 Hz), 7.20–7.27 (1H, m), 4.13 (2H, s), 3.62 (2H, s).^{13}C-NMR (100 MHz, $CDCl_3$) δ 186.8, 183.2, 172.7, 159.3, 149.8, 141.6, 137.0, 135.9, 134.6, 134.5, 134.4, 134.3, 133.1, 127.7, 127.3, 127.1, 126.7, 123.1, 122.7, 118.7, 55.5, 53.9.

Metal ion binding study by UV-vis and fluorescence spectroscopy. Chemosensor **1** or **2** (10^{-4} M) was added with different metal ions (10^{-4} M). All spectra were measured in 1.0 mL methaol–water solution (v/v = 4 : 1, 20 mM Hepes buffer, pH 7.0). The light path length of cuvette was 1.0 cm.

The pH dependence on Cu^{2+} binding in chemosensor 1 and 2 studied by UV-vis spectroscopy. Chemosensor **1** and **2** (10^{-4} M) was added with Cu^{2+} (10^{-4} M) in 1.0 mL methanol–water solution (v/v = 4 : 1, 20 mM buffer). The buffers were: pH 1–2, KCl/HCl; pH 2.5–4, KHP/HCl; pH 4.5–6, KHP/NaOH; pH 6.5–10 Hepes.

Determination of the binding stoichiometry and the stability constants K_a of Cu(II) binding in chemosensor 1 and 2. The binding stoichiometry of **1**-Cu^{2+} and **2**-Cu^{2+} complexes was determined by Job's plot experiments.[10] The absorbance at 473 nm was plotted against molar fraction of **1** or **2** under a constant total concentration. The concentration of the complex approached a maximum absorbance when the molar fraction was 0.5. These results indicate that both chemosensor **1** and **2** form a 1 : 1 complex with Cu^{2+}. The stability constants K_a of 1 : 1 **1**-Cu^{2+} and **2**-Cu^{2+} complexes were determined by the Benesi–Hilderbrand equation:[10]

$$1/\Delta A = 1/\Delta A_{sat} + 1/(\Delta A_{sat}\, K_a[Cu^{2+}]) \quad (1)$$

where ΔA is the absorbance difference at 473 nm and ΔA_{sat} is the maximum absorbance difference at 473 nm. The association constant K_a was evaluated graphically by plotting $1/\Delta A$ against $1/[Cu^{2+}]$. Typical plots ($1/\Delta$absorbance *vs.* $1/[Cu^{2+}]$ are shown in Fig. 8. Data were linearly fitted according to eqn 1 and the K_a value was obtained from the slope and intercept of the line. The K_a values of **1**-Cu^{2+} and **2**-Cu^{2+} complexes were 8470 M^{-1} and 18667 M^{-1}, respectively.

Acknowledgements

We gratefully acknowledge the financial supports of the National Science Council (ROC) and National Chiao Tung University.

Notes and references

1 (*a*) B. Valeur and I. Leray, *Coord. Chem. Rev.*, 2000, **205**, 3–40; (*b*) J. F. Callan, A. P. Silva and D. C. Magri, *Tetrahedron*, 2005, **61**, 8551–8588; (*c*) R. McRae, P. Bagchi, S. Sumalekshmy and C. J. Fahrni, *Chem. Rev.*, 2009, **109**, 4780–4827; (*d*) K. L. Haas and K. J. Franz, *Chem. Rev.*, 2009, **109**, 4921–4960.

2 (*a*) Y. Zheng, K. M. Gattas-Asfura, V. Konka and R. M. Leblanc, *Chem. Commun.*, 2002, 2350; (*b*) T. Gunnlaugsson, J. P. Leonard and N. S. Murray, *Org. Lett.*, 2004, **6**, 1557; (*c*) L. Zeng, E. W. Miller, A. Pralle, E. Y. Isacoff and C. J. Chang, *J. Am. Chem. Soc.*, 2006, **128**, 10; (*d*) Z. Xu, X. Qian and J. Cui, *Org. Lett.*, 2005, **7**, 3029; (*e*) X. Qi, E. J. Jun, L. Xu, S. Kim, J. S. J. Hong, Y. J. Yoon and J. Yoon, *J. Org. Chem.*, 2006, **71**, 2881; (*f*) N. Kaur and S. Kumar, *Dalton Trans.*, 2006, 3766; (*g*) N. Kaur and S. Kumar, *Chem. Commun.*, 2007, 3069; (*h*) J. Liu and Y. Lu, *J. Am. Chem. Soc.*, 2007, **129**, 9838; (*i*) Z. Xu, S. Kim, H. N. Kim, S. J. Han, C. Lee, J. S. Kim, X. Qian and J. Yoon, *Tetrahedron Lett.*, 2007, **48**, 9151; (*j*) W. Chen, X. Tu and X. Guo, *Chem. Commun.*, 2009, 1736–1738; (*k*) H. S. Jung, P. S. Kwon, J. W. Lee, J. Kim, C. S. Hong, J. W. Kim, S. Yan, J. Y. Lee, J. W. Lee, T. Joo and S. Kim, *J. Am. Chem. Soc.*, 2009, **131**, 2008–2012; (*l*) S. Wu, R. Huang and K. Du, *Dalton Trans.*, 2009, 4735–4740; (*m*) S. Wu and S. Liu, *Sens. Actuators, B*, 2009, **141**, 187–191.

3 (*a*) E. Kimura, S. Aoki, E. Kikuta and T. Koike, *Proc. Natl. Acad. Sci. U. S. A.*, 2003, **100**, 3731–3736; (*b*) Y. Mikata, M. Wakamatsu and S. Yano, *Dalton Trans.*, 2005, 545–550; (*c*) M. Royzen, A. Durandin, V. G. Young, N. E. Geacintov and J. W. Cannary, *J. Am. Chem. Soc.*, 2006, **128**, 3854–3855; (*d*) J. Wu, W. Liu, X. Zhuang, F. Wang, P. Wang, S. Tao, X. Zhang, S. Wu and S. Lee, *Org. Lett.*, 2007, **9**, 33–6; (*e*) S. Huang, R. J. Clark and L. Zhu, *Org. Lett.*, 2007, **9**, 4999–5002; (*f*) K. Komatsu, Y. Urano, H. Kojima and T. Nagano, *J. Am. Chem. Soc.*, 2007, **129**, 13447–13454; (*g*) W. Jiang, Q. Fu, H. Fan and W. Wang, *Chem. Commun.*, 2008, 259–261; (*h*) Z. Liu, C. Zhang, Y. Li, Z. Wu, F. Qian, X. Yang, W. He, X. Gao and Z. Guo, *Org. Lett.*, 2009, **11**, 795–798; (*i*) X. Chen, J. Shi, Y. Li, F. Wang, X. Wu, Q. Guo and L. Liu, *Org. Lett.*, 2009, **11**, 4426–4429; (*j*) L. Xue, C. Liu and H. Jiang, *Chem. Commun.*, 2009, 1061–1063.

4 (*a*) G. E. Tumambac, C. M. Rosencrance and C. Wolf, *Tetrahedron*, 2004, **60**, 11293; (*b*) J. L. Bricks, A. Kovalchuk, C. Trieflinger, M. Nofz, M. Büschel, A. I. Tolmachev, J. Daub and K. Rurack, *J. Am. Chem. Soc.*, 2005, **127**, 13522; (*c*) J. P. Summer and R. Kopelman, *Analyst*, 2005, **130**, 528–533; (*d*) Y. Xiang and A. Tong, *Org. Lett.*, 2006, **8**, 1549–1552; (*e*) S. Bae and J. Tae, *Tetrahedron Lett.*, 2007, **48**, 5389–5392.

5 (*a*) F. Monteil-Rivera and J. Dumoncean, *Anal. Bioanal. Chem.*, 2002, **374**, 1105–1112; (*b*) N. Kaur and S. Kumar, *Tetrahedron Lett.*, 2008, **49**, 5067–5069; (*c*) X. Wang, W. Zheng, H. Lin, G. Liu, Y. Chen and J. Fang, *Tetrahedron Lett.*, 2009, **50**, 1536–1538.

6 H. Irving and R. J. P. Williams, *J. Chem. Soc.*, 1953, 3192.

7 (*a*) H. Miyaji and J. L. Sessler, *Angew. Chem., Int. Ed.*, 2001, **40**, 154–157; (*b*) X. Peng, Y. Wu, J. Fan, M. Tian and K. Han, *J. Org. Chem.*, 2005, **70**, 10524–10531; (*c*) E. Ranyuk, C. M. Douaihy, A. Bessmertnykh, F. Denat, A. Averin, I. Beletskaya and R. Guilard, *Org. Lett.*, 2009, **11**, 987–990.

8 S. Kumar, V. Luxami and A. Kumar, *Org. Lett.*, 2008, **10**, 5549–5552.

9 (*a*) M. Mameli, M. C. Aragoni, M. Arca, M. Atzori, A. Bencini, C. Bazzicalupi, A. J. Blake, C. Caltagirone, F. A. Devillanova, A. Garau, M. B. Hursthouse, F. Isaia, V. Lippolis and B. Valtancoli, *Inorg. Chem.*, 2009, **48**, 9236–9249; (*b*) F. Zapata, A. Caballero, A. Espinosa, A. Tarraga and P. Molina, *Inorg. Chem.*, 2009, **48**, 11566–11575; (*c*) F. Zapata, A. Caballero, A. Espinosa, A. Tarraga and P. Molina, *J. Org. Chem.*, 2010, **75**, 162–169.

10 T. Kao, C. Wang, Y. Pan, Y. Shiao, J. Yen, C. Shu, G. Lee, S. Peng and W. Chung, *J. Org. Chem.*, 2005, **70**, 2912–2920.

11 M. Meyer, L. Fremond, E. Espinosa, R. Guilard, Z. Ou and K. M. Kadish, *Inorg. Chem.*, 2004, **43**, 5572–5587.

12 (*a*) G. Speier, J. Csihony, A. M. Whalen and C. G. Pierpont, *Inorg. Chim. Acta*, 1996, **245**, 1–5; (*b*) S. Roy, B. Sarkar, D. Bubrin, M. Niemeyer, S. Zalis, G. K. Lahiri and W. Kaim, *J. Am. Chem. Soc.*, 2008, **130**, 15230–15231.

